

# Experimental report

29/08/2024

**Proposal:** 9-12-709

**Council:** 4/2023

**Title:** Stabilization of ligand-coated non-polar nanoparticle dispersions by addition of molecular additives

**Research area:** Soft condensed matter

**This proposal is a new proposal**

**Main proposer:** Bart-Jan NIEBUUR

**Experimental team:** Bart-Jan NIEBUUR

Thomas KISTER

Tobias KNAPP

**Local contacts:** Olga MATSARSKAIA

Lionel PORCAR

**Samples:** C18H34S-coated Au nanoparticles in decane

Instrument	Requested days	Allocated days	From	To
D22	1	1	30/08/2023	31/08/2023
D33	1	0		

## Abstract:

Ligand-stabilized gold nanoparticles are promising building blocks for materials with well-defined structures and properties. Their colloidal stability is limited, even though stability is essential for their combination with other components and the definition of superstructures that define functionality. Molecular additives may strongly change particle stability, even at low concentrations, because they affect the conformation of the ligands inside the shells. Preliminary small-angle X-ray scattering (SAXS) showed an improved nanoparticle stability in the presence of cyclic amines and thiols as additives, suggesting that they are accumulated inside the ligand shell. However, due to the small differences in electron densities between organic components, SAXS cannot be used to investigate the shell structure directly. Therefore, we propose small-angle neutron scattering to investigate the distribution of additive molecules inside and around the shell. The results will help us to understand the mechanisms behind the improved nanoparticle stability, as well as to direct the search for additional additives.

Small ligand-stabilized apolar gold nanoparticles (AuNPs) are a class of materials with a high potential for use in various applications, such as catalysis, photovoltaics, printable electronics and quantum-dot enhanced sensors and displays. Their colloidal stability in organic solvents is an important property, as agglomeration impedes effective processing or their functionality in applications. Colloidal stability is accommodated by steric effects of the ligand shell, which prevents agglomeration due to der Waals interactions between the Au cores [1]. However, it has been shown that a disorder-to-order transition of the ligand shell may lead to nanoparticle agglomeration at low temperatures, governed by short-ranged entropic and enthalpic interactions inside the shell, which, therefore, depends strongly on its composition [2]. For example, our previous work demonstrated the possibility to tune the colloidal stability of hexadecanethiol (HDT)-coated AuNPs dispersed in solvent mixtures [3].

In a next step, we explore the use of molecular additives to improve the colloidal stability of AuNPs. Especially cyclic molecules, which cannot align with linear ligands while intercalating the ligand shell, are expected to stabilize the disordered state of the ligand shell, thereby improving the AuNP colloidal stability. For this, we chose the amine-based additives pyrrolidine (R5N) and azonane (R9N), and sulfide-based additives tetrahydrothiophene (R5S) and thionane (R9S) to investigate the effect of additive molecular size and affinity to the Au core surface. Small-angle X-ray scattering (SAXS) was used to quantify the colloidal stability of 4 nm AuNPs coated with HDT ligands dispersed in *n*-decane, while small-angle neutron scattering (SANS) provided information on the structure and composition of their ligand shell. Lastly, molecular dynamics (MD) simulations provided understanding of interactions on the molecular level leading to the stabilizing effect of additives molecules.

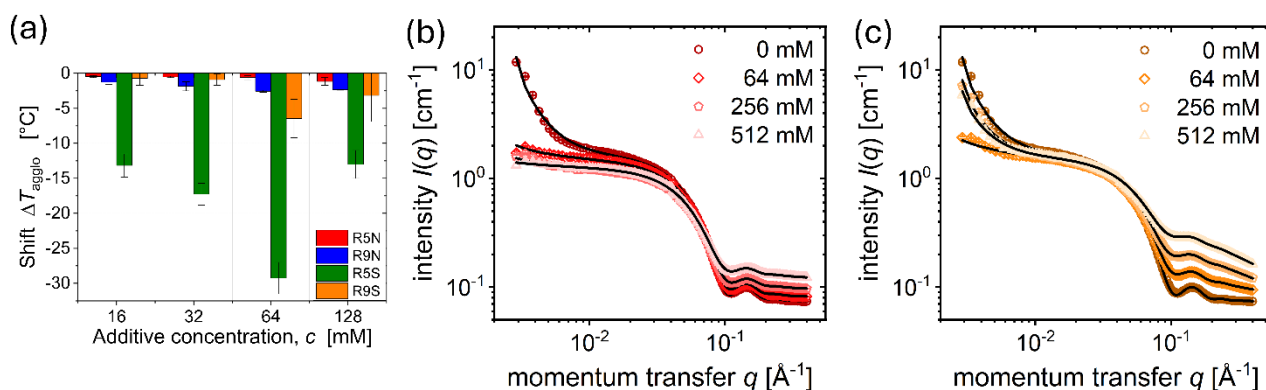


**Figure 1.** (a) Changes in  $T_{\text{agglo}}$  of HDT-coated 4 nm AuNPs dispersed in *p*-decane in the presence of all investigated additive molecules at different concentrations as compared to  $T_{\text{agglo}}$  of AuNPs dispersed in pure *p*-decane. (b) SANS patterns of AuNPs dispersed in *d*-decane in the presence of different concentrations of R5N additives, and (c) in the presence of several concentrations of R9S additives. In (b) and (c), the black lines are model fits using eq. 1.

Temperature-dependent SAXS measurements provided the agglomeration temperature ( $T_{\text{agglo}}$ ) of AuNP dispersed at a concentration of  $2.5 \text{ mg ml}^{-1}$  in hydrogenated decane (*p*-decane) in dependence on additive type and concentration [4]. The shift of  $T_{\text{agglo}}$  as compared to that of AuNPs dispersed in pure *p*-decane,  $\Delta T_{\text{agglo}}$ , is shown in Figure 1a. All investigated additives showed a negative  $\Delta T_{\text{agglo}}$  at all concentrations, i.e., they stabilized the dispersions. R5S showed the strongest stabilizing effect with  $\Delta T_{\text{agglo}} = -29 \text{ }^\circ\text{C}$  and a concentration of 64 mM. The stabilizing effect of R9S was weaker,  $\Delta T_{\text{agglo}} = -6.5 \text{ }^\circ\text{C}$  at 64 mM, while both amine-based additives had an only marginal effect: R9N lowered  $T_{\text{agglo}}$  by  $2.5 \text{ }^\circ\text{C}$  at 64 mM, and R5N by  $1.1 \text{ }^\circ\text{C}$  at 128 mM. Two effects leading to the

stabilizing effect are conceivable: Additives may intercalate the shell and physisorb, acting like a surfactant, or chemisorb to change the structure of the ligand shell. Both change the composition and structure of the ligand shell, which may reduce the temperature at which the ligands order. The magnitude of this effect will depend on the number as well as position of additives inside the shell.

To investigate the influence of additives on the ligand shell structure, SANS was employed to quantify the composition of the ligand shell. For this, HDT-coated AuNPs were dispersed in deuterated *n*-decane (*d*-decane) with concentrations of 0, 64, 256 and 512 mM of added additives, and measured at 35 °C, i.e., in the dispersed state for all samples. To ensure good statistics, a particle concentration of 10 mg ml<sup>-1</sup> was chosen. A *q* range from 0.003-0.4 Å<sup>-1</sup> was covered with sample-detector distances of 17 m and a neutron wavelength of 6 Å. The sample was mounted in quartz glass cuvettes with a thickness of 2 mm. The signal of the empty cuvettes was subtracted from the data.

Figure 1b and c present exemplary SANS patterns of AuNP dispersions in the presence of R5N and R9S additive molecules, respectively. In all cases, the scattering patterns feature a shoulder above ~0.02 Å<sup>-1</sup>, which results from scattering at the particle shells and cores. For R9S containing AuNP dispersions, a second shoulder is present at high *q*-values that match with those of the decays observed in additive solutions in the absence of AuNPs (not shown). Therefore, this decay results from scattering at composition fluctuations in the solvent on molecular length scales. Additionally, weak forward scattering is observed in some cases, pointing to weak agglomeration of the NPs. To account for these contributions, the scattering curves were modelled using the expression

$$I(q) = I_P(q) + I_{PCS}(q) + I_{OZ}(q) + I_{bkg} \quad (1)$$

which combines a Porod function,  $I_P(q)$ , a form factor of polydisperse core-shell particles,  $I_{PCS}(q)$ , and an Ornstein-Zernike structure factor,  $I_{OZ}(q)$ . Additionally, a constant term,  $I_{bkg}$ , is added to account for incoherent background scattering. During fitting, the composition and structure of the solvent matrix was assumed not to be affected by the presence of AuNPs. Standard procedures were applied to account for the divergence and wavelength distribution of the neutron beam.

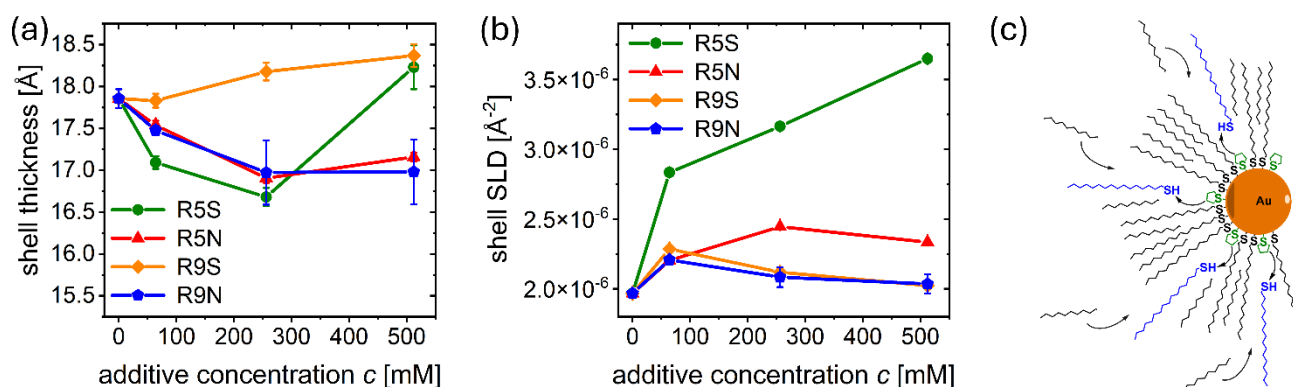


**Figure 2.** Results from fitting the SANS patterns. (a) shell thickness,  $t_s$ , and (b) shell SLD,  $SLD_s$ . (c) Sketch of the hypothesized ligand exchange mechanism, exemplified for AuNP dispersions containing R5S additive molecules. R5S replaces HDT on the Au core surfaces, allowing for a stronger ligand solvation by *d*-decane.

The shell thickness,  $t_s$ , resulting from the fits, is shown in Figure 2a in dependence on additive concentration. In the absence of additive molecules, it was ~18 Å, which is slightly below the value expected for fully stretched HDT ligands [3]. At low additive concentrations,  $t_s$  decreased for all additive types, albeit marginally. At higher concentrations, this trend continued for both amine-based additives, while  $t_s$  in the presence of sulfide-based additives slightly increased. At the highest

measured concentration of 512 mM, it was 18-19 Å for both sulfide-based additives and ~17 Å for both amine-based additives.

Figure 2b presents the scattering length density (SLD) of the ligand shells,  $SLD_s$ . In the absence of additive molecules, it was  $\sim 1.97 \cdot 10^{-6} \text{ \AA}^{-2}$ . Under the assumption that the molecular volumes of HDT and *d*-decane inside the shell assume the same values as their bulk values, this corresponds to a shell composition of 56:44 n/n HDT/*d*-decane. With increasing additive concentration,  $SLD_s$  increased for all additive types. As HDT as well as all additive molecules were hydrogenated, an increase in  $SLD_s$  implies, that the fraction of *d*-decane inside the shell upon addition of additives increases. A partial exchange of HDT ligand molecules by the much smaller additive molecules on the Au core surface is conceivable, as it creates more space for *n*-decane molecules to enter the shell (Figure 1c).

At the highest measured concentration of 512 mM, R5S led to the largest  $SLD_s$  of  $\sim 3.65 \cdot 10^{-6} \text{ \AA}^{-2}$ , while for R5N it was  $\sim 2.33 \cdot 10^{-6} \text{ \AA}^{-2}$ . The larger R9S and R9N only caused a marginally larger  $SLD_s$  of  $2.03 \cdot 10^{-6} \text{ \AA}^{-2}$  at 512 mM. Therefore, an influence of both additive size and affinity to the Au core surfaces is discernible. The smaller R5S and R5N replace more HDT ligands than R9S and R9N, creating more space for *n*-decane to enter the shell and solvate the remaining HDT ligands. This effect is more pronounced for R5S than for R5N. While the Au-R5S and Au-HDT binding energies are similar, that of Au-R5N is significantly smaller, and less HDT ligands are replaced by R5N. Furthermore, this picture is compatible with the behavior of  $t_s$ : The marginal changes imply, that the dimensions of the shell are set by HDT ligands for all additive types and concentrations.

Complementary MD simulations provided additional insights into the influence of additive size [4]. For this, we calculated the potential of mean force between both sulfide-based additives and the HDT-coated AuNPs by gradually moving a single additive away from the Au core surface. It was found that R5S had favorable interaction with the AuNP near the core, while for R9S the interaction was unfavorable throughout the entire shell. Therefore, R5S experiences less steric hindrance while approaching the Au core surface than the larger R9S, explaining the observed effects.

The picture that emerges is the following: The replacement of HDT ligands by R5S allows more *n*-decane to enter the shell as compared to the additive-free system. The resulting increased solvation of the remaining ligands strengthens steric repulsion [5], thereby stabilizing the colloidal stability of AuNPs. Similarly, R5N replaced HDT ligands on the Au core surfaces. However, less ligands were replaced due to the smaller Au-R5N binding energy, which led to a significantly smaller improvement of the AuNP colloidal stability. HDT ligands were only scarcely replaced by the larger R9S and R9N due to steric constraints. Possibly, physisorption of these cyclic additives inside the ligand shell, hampering alignment of the linear ligands to suppress their disorder-to-order transition, may play a significant role in the improved colloidal stability in the presence of these ligands. Future complementary MD simulations and experiments will investigate this further.

We thank Dr. Olga Matsarskaia for excellent support during the measurements.

[1] Kister, T.; Monego, D.; Mulvaney, P.; Widmer-Cooper, A.; Kraus, T. *ACS Nano*, **2018**, *12*, 5969-5977. [2] Monego, D.; Kister, T.; Kirkwood, N.; Doblaz, D.; Mulvaney, P.; Kraus, T.; Widmer-Cooper, A. *ACS Nano*, **2020**, *14*, 5278-5287. [3] Hasan, R. H.; Niebuur, B.-J.; Siebrecht, M.; Kuttich, B.; Schweins, R.; Widmer-Cooper, A.; Kraus, T. *ACS Nano*, **2023**, *17*, 9302-9312. [4] Knapp, T. V.; Hasan, R. H.; Niebuur, B.-J.; Widmer-Cooper, A.; Kraus, T. *submitted*. [5] Shah, P. S.; Holmes, J. D.; Johnston, K. P.; Korgel, B. A. *J. Phys. Chem. B*, **2002**, *106*, 2545-2551